PROCEEDINGS OF SCIENCE

# Physics and effects of relativistic SEPs/GLEs

**Alexander Mishev**[a,b,*]

[a] *Sodankylä Geophysical Observatory, University of Oulu, Finland*

[b] *Space Physics and Astronomy Research Unit, University of Oulu, Finland*

*E-mail:* alexander.mishev@oulu.fi

Systematic study of relativistic solar energetic particles provides key information about various processes, such as production and acceleration of energetic particles at the Sun and the interplanetary medium, interactions of energetic particles with magnetic fields in the heliosphere i.e. probing the electromagnetic and plasma conditions of the heliosphere, assessment of their terrestrial and space weather effects. Following solar eruptive processes, such as solar flares and/or coronal mass ejections solar ions are accelerated to a high-energy range. In the majority of cases, the maximum energy of the accelerated solar ions is several tens of MeV/nucleon, but in some cases, it exceeds 100 MeV/nucleon or even reaches GeV/nucleon range. In this case, the energy is enough high, so that solar ions generate an atmospheric cascade in the Earth's atmosphere, whose secondary particles reach the ground, eventually registered by ground-based detectors, specifically neutron monitors. This particular class of events is known as ground-level enhancements (GLEs). Here we report recent achievements related to the physics of relativistic SEPs/GLEs, their observations, and the related terrestrial and space weather effects.

*27th European Cosmic Ray Symposium - ECRS*
*25-29 July 2022*
*Nijmegen, the Netherlands*

*Speaker





PoS(ECRS)016

## 1. Introduction

It is known that occasionally following solar eruptive processes such as solar flares and/or coronal mass ejections (CMEs) our nearest star - the Sun accelerates particles, namely protons, electrons, and heavier nuclei, the latter specifically He-Fe, from a few keV up to the GeV energy range [1]. Those particles observed in the interplanetary space as well as in the vicinity of the Earth are commonly referred to as solar energetic particles (SEPs) [2].

Methodological studies of SEPs provide the necessary basis to reveal fundamental questions related to the ion acceleration on the Sun, where a specific interest is paid to particles with energy reaching about GeV/nucleon or even greater values, that is strong and relativistic ones, which can produce secondary particles in the Earth's atmosphere eventually registered by convenient ground-based detectors, *e.g.* neutron-monitors (NMs) [3]. This type of SEP events is known as ground level enhancements (GLEs) [4, 5]. Moreover, SEPs, specifically those leading to GLEs, are among the important aspects of solar-terrestrial physics, as well as are closely related to important space weather effects such as the enhanced atmospheric ionization, complex radiation environment specifically at flight altitudes and near space [6–8]. Here we discuss several recent achievements related to the physics, terrestrial and, space weather effects of relativistic SEPs/GLEs.

## 2. Progress in physics of relativistic SEPs/GLEs

Over the last two decades, the ruling paradigm of SEP origin was that they are produced by the sudden release of accumulated magnetic energy during solar eruptions, specifically, those accelerated at flares are referred to as impulsive events, while particles accelerated by near-Sun CME-driven shocks as gradual events Fig.1 1 [1, 9]. The gradual events typically lasted several days and exhibit larger fluence compared to the impulsive ones. They are proton-rich, had average Fe/O ratios of 0.1, and are associated with type II radio bursts. The impulsive events lasted a few hours and usually possess smaller fluences, are electron-rich, and associated with type III radio bursts.

Even good progress in understanding the SEP acceleration was achieved, yet there are several open questions, specifically about the relative role of flares and CME-driven shocks in the particle energization and to explain the prolonged X-ray and $\gamma$- emissions, results by electrons colliding with ambient ions for the former and ions interacting with the dense layers above the solar surface for the latter [10]. Note, that GLEs exhibit shorter duration compared to gradual SEP events and are usually accompanied by both strong solar flares and fast and wide CMEs. Morphological studies suggest two components: a prompt component (PC) associated with solar flares, typically beam-like, that is with narrow angular distribution, which is followed by a delayed component (DC) resulting from shock/CME acceleration of particles [11], naturally with isotropic-like angular distribution. An important feature is the different spectral shapes of the PC and DC, usually approximated with exponent and power-law in energy/rigidity, respectively, yet different spectral shapes are also proposed.

Recently, based on on-situ observations and phenomenological studies, in fact, an evolution of a previously proposed mechanism was proposed by several teams [12, 13]. It was suggested that both mechanisms appear to contribute, with one accelerating mechanism operating in the

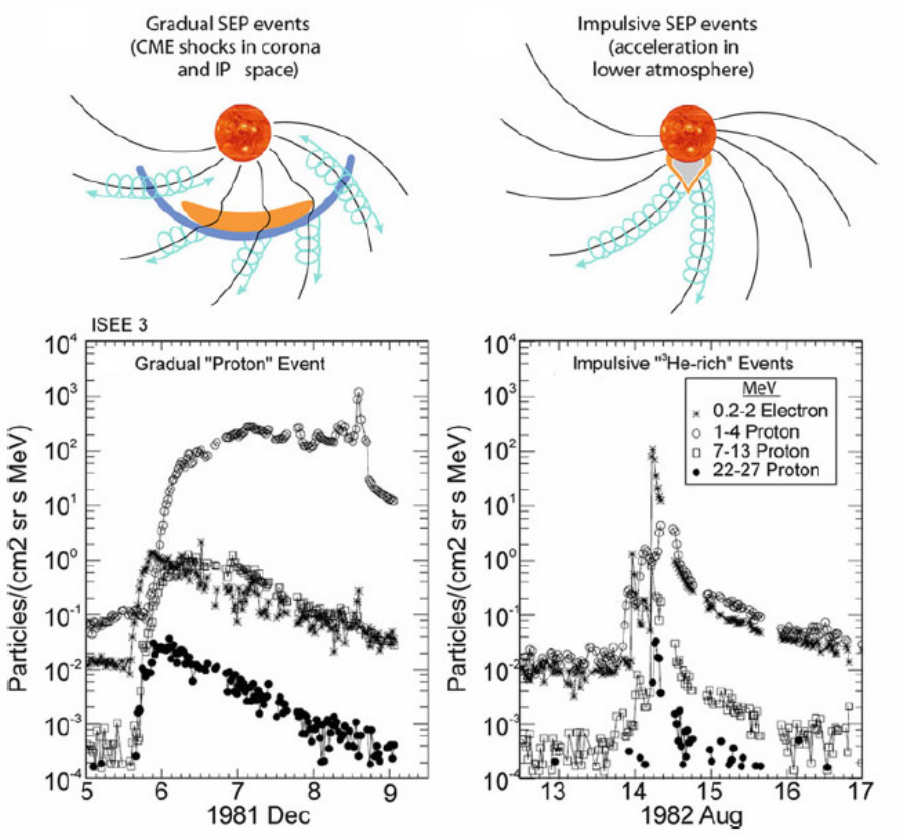


**Figure 1:** Long-ruled paradigm of flare/impulsive–CME shock/gradual acceleration of SEPs. The upper left panel depicts gradual SEP events resulting from diffusive acceleration at CME-driven shocks. The upper right panel depicts impulsive SEP events which are produced by solar flares. Accordingly, the lower panels represent gradual and impulsive SEP events. Adapted from [1] permission for reuse from author and publisher Springer according to license CC BY 4.0.

flare while the other operates at the CME-driven shock, including re-acceleration of remnant flare suprathermals by shockwaves or from the interaction of CMEs. For instance, as depicted in Fig. 2 the impulsive phase of the solar flare comprises an outburst, causing also a global coronal wave and during the eruption as such, the PC of particles is accelerated, comprising partially also the seed population of the re-accelerating particles. Some of the particles can be trapped and lately eventually reaccelerated. The partial trapping of the relativistic SEPs can be it in the loops at low altitudes and/or in the flux rope rising above, a plausible scenario to explain a long-duration $\gamma$-emission form pion-decay.

The injection of relativistic protons occurs upon the CME arrival at the top sections of helmet streamers and concurrently with the lateral expansion of CME at its right flank, the latter responsible for the prolonged emission, yet the shocks can contribute to the DC, specifically for low-energy populations at several solar radii.

Such hybrid mechanisms are plausible explanations of particle acceleration and long-duration $\gamma$-emission and extended radio source, the latter produced by the rising CME at different coronal altitudes and can be regarded as an evolution of the scenario proposed by Mandzhavidze–Ramaty

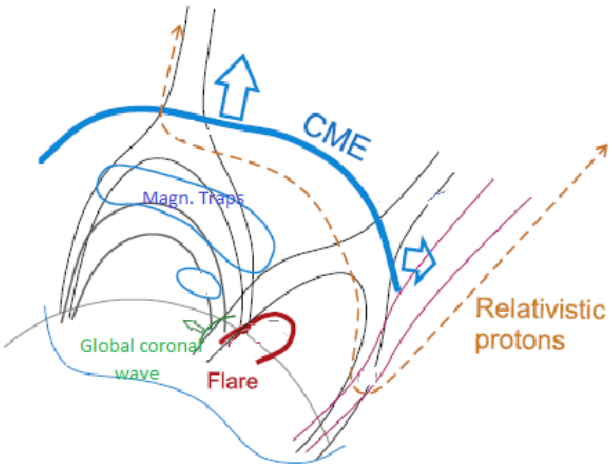


**Figure 2:** Hybrid mechanism:flare-CME-particle trapping-reacceleration of SEP energetization.

[14] and supported by morphological studies [15, 16] and recent observations/models [13, 17] .

## 3. Registration and analysis of GLEs using NM records

When a primary CR enters in the atmosphere it induces an extensive air shower, that is the primary interacts with an atmospheric constituent and produces a large variety of secondaries, accordingly, the secondaries also collide with atmospheric constituents, in turn producing other, i.e., the next generation of particles. Each collision adds a certain amount of particles, leading to the development of a complicated nuclear-electromagnetic-meson cascade known as an extensive air shower (EAS). A specifically designed detector, that is NM can register mostly the hadron component of the EAS Fig. 3a, where the minimum energy necessary to give a signal in the station is about 300 MeV/n for the polar high-altitude NMs and 430 MeV/n for low rigidity cut-off stations at sea level respectively [18].

It was shown that GLEs can be studied with ground-based instruments, namely NMs [19, 20]. Stations at different geographic regions are sensitive to a different part of the SEP spectra and arrival direction [21]. Since GLEs occur sporadically and naturally differ from each other in spectra, particle flux, anisotropy, duration, and time evolution, they are studied on a case-by-case basis [22].

For reliable analysis of NM records, it is necessary to possess enough NM stations [20]. The methods for analysis of GLEs using NM data are based on modeling the global NM network response and unfolding $n$ model parameters over the experimental records of $m$ NMs [23, 24].

The response of each NM is computed by integral of the product of the primary CR spectrum $J(P,t)$ with the specific NM yield function $S(P,h)$, that is the count rate of an NM at a given altitude $h$ and time $t$ is expressed as:

$$N(P_c,h,t) = \sum_i \int_{P_c}^{\infty} S_i(P,h)\, J_i(P,t)\, dP \tag{1}$$

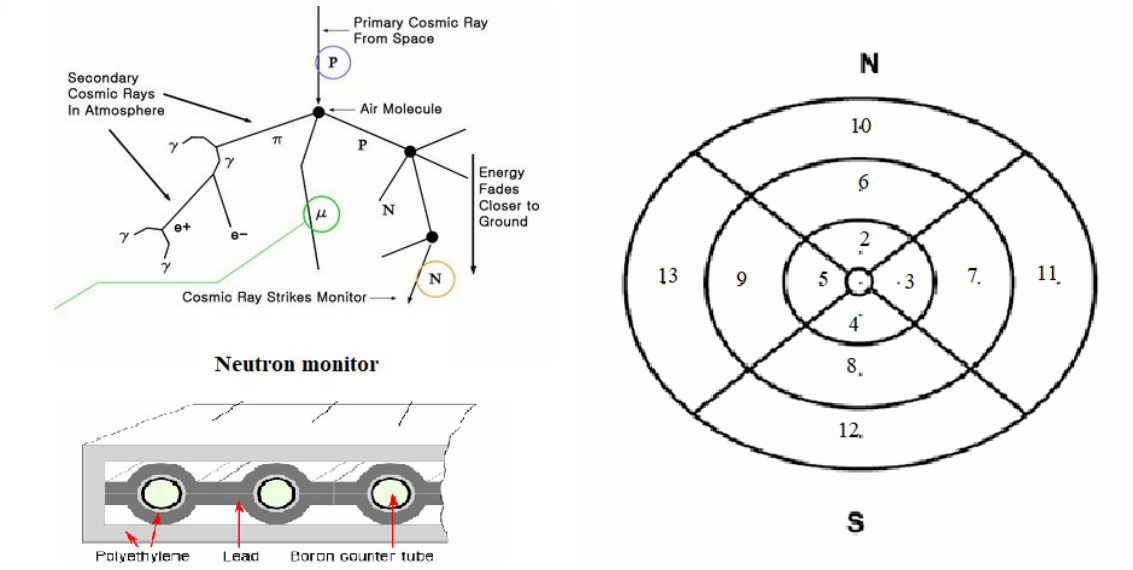


**(a)** Sketch of extensive air shower induced by primary CR**(b)** Segments of the sky over the response of an NM station proton and the registration of mostly hadron secondaries by ais integrated during the modeling-unfolding procedure. NM.

**Figure 3:** Registration and analysis of CRs with NMs.

where $P_c$ is the local geomagnetic rigidity cut-off, $h$ is the atmospheric depth (or altitude), $S_i(P,h)$ [m$^2$ sr] is the NM yield function for primaries of particle type $i$ (protons and/or $\alpha$-particles), $J_i(P,t)$ [GV m$^2$ sr sec]$^{-1}$ is the rigidity spectrum of the primary particle of type $i$ at time $t$ [25]. We emphasize that the modeling should reproduce the stations with maximal and significant count rate increases as well as with marginal or null count rate increases [23].

Here we employed a method based on validated by direct space-born measurements new generation NM yield function, [26, 27] and robust flexible optimization, that is with variable regularization and damper of the process, including local root extractor [28–30] within Levenberg-Marquardt method [31, 32]. We would like to emphasize that the new generation of NM yield function is in excellent agreement with experimental records and models [33, 34] and it is the best situated for GLE analysis [35]. The method was recently verified by direct space-born measurements and was used for the analysis of a plethora of GLEs [36–40].

Here, the relative count rate increase of a given NM during GLE is modeled using:

$$\frac{\Delta N(P_{\rm cut})}{N(t)} = \frac{\sum_i \sum_k \int_{P_{\rm cut}}^{P_{\rm max}} J_{{\rm sep}_{\rm i}}(P,t) S_{i,k}(P) G_i(\alpha(P,t)) A_i(P) dP}{\sum_i \int_{P_{\rm cut}}^{\infty} J_{{\rm GCR}_{\rm i}}(P,t) S_i(P) dP} \tag{2}$$

where $N(t)$ is the count rate due to GCR, $\Delta N(P_{\rm cut})$ is the count rate increase due to solar particles. $J_{\rm sep}$ is the rigidity spectrum of SEPs $i$ (proton or $\alpha$-particle), $J_{{\rm GCR}_{\rm i}}(P,t)$ is the rigidity spectrum of the $i$ component (proton or $\alpha$-particle, etc...) of GCR at given time $t$, $G(\alpha(P,t))$ is the pitch angle distribution (PAD), note for GCRs the angular distribution is assumed to be isotropic, A(P) is a discrete function with $A(P)$=1 for allowed trajectories and $A(P)$=0 for forbidden trajectories.

Function $A$ is derived during the asymptotic cone computations. $P_{\text{cut}}$ is the minimum rigidity cut-off of the station, accordingly, $P_{\text{cut}}$ is the maximum rigidity of SEPs considered in the model, whilst for GCR $P_{\text{max}}= \infty$. $S_k$ is the NM yield function for vertical and for oblique incidence SEPs from various segments Fig. 3b, where 1 corresponds to vertical incidence, 2–5 for SEPs inclined of 15 degrees and azimuth angles with steps of 90 degrees, segments 6–9 and 10–13 correspond to an inclination of 30 and 45 degrees with the same azimuthal incidence as the above-mentioned segments, respectively. The contribution of oblique SEPs to NM response is particularly important for modeling strong and/or very anisotropic events [41], while for weak and/or moderately strong events it is possible to consider only vertical ones and using $S_k$ for an isotropic case, which considerably simplifies the computations [42].

In Equation 2 the GCR spectrum is parameterized employing the force-field model [43] using an approximation of the local interstellar spectrum by [44], accordingly the solar modulation parameter is computed similarly to [45].

The method involves the following consecutive steps: computation of asymptotic viewing directions and rigidity cut-off of all NMs used for the data analysis; making an initial guess of the optimization procedure [42] similarly to [46] and performing the optimization itself, that is using modeled and recorded NM responses over a selected space of unknown parameters to determine the spectra, PAD and apparent source position of the source.

Here, the magnetospheric computations that is the rigidity cut-off and asymptotic directions of each NM station used in the analysis, were performed using an open source tool OTSO [47] employing a combination of the IGRF geomagnetic model as the internal field model e.g. [48] and the e.g. Tsyganenko 89 model as the external field [49], explicitly considering the measured $K_p$ index prior and during the event. This combination of models provides reasonable precision and straightforward computation of the rigidity cut-offs and asymptotic directions necessary for the NM data analysis [50, 51]. Note, that use of later Tsyganenko models should be considered during periods of intense geomagnetic activity (e.g. periods of Kp index above 6), since the TSY 89 is not recommended to be employed in such cases.

We emphasize that the employed inverse problem solution method is somehow interpolation between the Gauss–Newton and the method of gradient descent, but benefiting because the floating damper and flexible regularization to obtain reliable solutions even if it starts far from the final minimum [28, 52]. In addition, because the derived spectra and mainly PADs are sensitive to apparent source assessment [53], we routinely compute and build the distribution of the sum of variances for the best-fit solutions vs. geographic coordinates, obtained by forward modeling over all the possible apparent source positions, that is we are performing verification of the derived SEP characteristics [54].

A notable example of the application of the described method is the analysis of GLE # 71, occurred on 17 May 2012. It followed active processes in the active region NOAA 11476, namely a CME and a moderately strong flare (class M5.1). At Earth, the worldwide NM network recorded a weak enhancement, and greater signals were recorded by APTY, OULU, and SOPO/SOPB NMs. The majority of the NMs exhibited marginal count rate increases, therefore a large anisotropy of the arriving SEPs, specifically during the event onset, was implied. This event was extensively studied [10, 15, 25, 55]. An example of several derived spectra and PADs is shown in Fig. 4.

The best fit is obtained using a modified power-law rigidity spectrum:

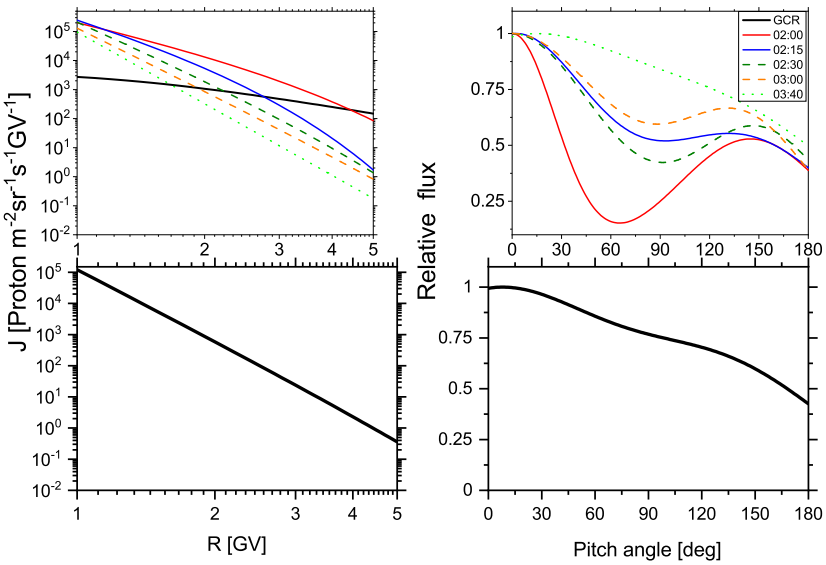


**Figure 4:** Top panels: derived SEP rigidity spectra (left panel) and PADs (right panel) during selected periods of GLE # 71. Bottom panels: event averaged SEP spectra (left) and PAD (right) during GLE # 71.

$$J_{||}(P) = J_0 P^{-(\gamma+\delta\gamma(P-1))} \tag{3}$$

where $J_{||}(P)$ is the particle flux with given rigidity $P$ in [GV] arriving from the Sun along the axis of symmetry, which is defined by the geographic coordinate angles $\Psi$ and $\Lambda$ (latitude and longitude). In Eq. 3, $\gamma$ is the power-law spectral exponent at rigidity P = 1 GV, accordingly $\delta\gamma$ is the rate of the spectrum steepening. The angular distribution of the arriving SEPs is depicted by complicated pitch angle distribution (PAD) Eq. 4 with a shape similar to that considered by [23], namely superposition of two Gaussians:

$$G(\alpha(P)) \sim exp(-\alpha^2/\sigma_1^2) + B * exp(-(\alpha - \alpha^{'})^2/\sigma_2^2) \tag{4}$$

where $\alpha$ is the pitch angle, $\sigma_1$ and $\sigma_2$ are parameters corresponding to the width of the pitch angle distribution, $B$ and $\alpha^{'}$ are parameters corresponding to the contribution of the second Gaussian, including direction nearly opposite to the derived axis of symmetry. Note, at and below P=1 GV, the Eq. 3 is slightly modified in order to avoid discontinuity. In general, here we distinguish three phases of the event: initial (01:50–02:25 UT) with a relatively hard spectrum and constant increase of SEP flux accompanied by complicated PAD; main phase (02:25–03:05 UT), with a steady softening of the SEP spectra and decrease of the SEP with corresponding decrease of the steepening $\delta\gamma$, and late phase of the event (after 03:05 UT), characterized with a pure power-law spectrum and nearly isotropic PAD. Here we emphasize that the initial and main phases of the event correspond to the PC, while the late phase to the DC. The transition of the main to the late phase of the event can be attributed somehow to trapping-reacceleration of part of the firstly accelerated protons as discussed in Section 2.

In addition, a very good agreement of the derived fluence and PAD during GLE # 71 with the direct measurements by PAMELA space-probe was achieved, including the complicated angular distribution [55, 56] . Besides, good agreement with SOHO/EPHIN measurements in the energy range 300-700 MeV/nucleon fitted with pure power-law was achieved [57]. Therefore, the employed method for analysis of NM data is somehow verified by direct measurements.

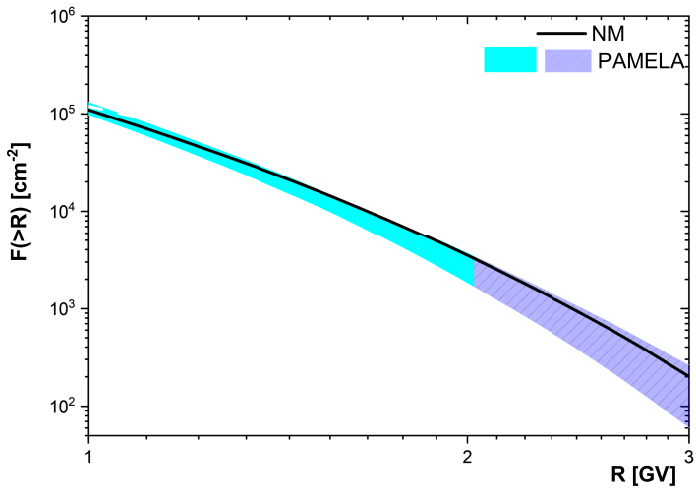


**Figure 5:** Integral SEP fluence during GLE 71 on May 17, 2012 computed using NM and PAMELA data reconstructions as denoted in the legend. The blue-filled and hatched area corresponds to the PAMELA data up to 2 GV and the corresponding data extrapolation above 2 GV respectively.

## 4. Space weather and terrestrial effects during relativistic solar particle events

During GLEs the increased intensity of CRs result in important space weather issues, specifically at flight altitudes [58], specifically on polar intercontinental flights, where the geomagnetic shielding is marginal. Over the last two decades following the progress of hadron interaction models and the corresponding Monte Carlo simulation tools, several models aiming at assessment of the absorbed dose (ambient dose equivalent, effective dose, ambient dose) at flight altitudes, henceforth exposure to radiation or simply exposure have been developed [59–61], which nicely agree with each-other within about 10–20 % [62]. Though, an important uncertainty, up to an order of magnitude, in the computation of the exposure during GLEs was reported [53, 63] mostly due to the considered SEP spectra, i.e., input for the models.

A convenient numerical model for computation of the exposure is based on pre-computed yield functions [64, 65]. In the model, the effective dose rate at a given atmospheric altitude (depth) $h$ induced by a primary CR particle is computed by integral of the product of the CR particle spectrum with the corresponding yield function:

$$E(h,T,\theta,\varphi) = \sum_i \int_{T(P_{cut})}^{\infty} \int_{\Omega} J_i(T) Y_i(T,h) d\Omega(\theta,\varphi) dT, \tag{5}$$

where $J_i(T)$ is the differential energy spectrum of the primary CR arriving at the top of the atmosphere for the $i-$th component of CRs (proton or $\alpha-$particle) and $Y_i$ is the corresponding effective dose yield function. The integration is over the kinetic energy $T$ above $T(P_{cut})$, which is defined by the local cut-off rigidity $P_{cut}$ and over the sold angle $\Omega$.

The effective dose yield function $Y_i$ is defined as:

$$Y_i(T,h) = \sum_j \int_{T^*} F_{i,j}(h,T,T^*,\theta,\varphi) C_j(T^*) dT^* \tag{6}$$

where $C_j(T^*)$ is the fluence to effective dose conversion coefficient for a secondary particle of type $j$ (neutron, proton, $\gamma$, $e^-$, $e^+$, $\mu^-$, $\mu^+$, $\pi^-$, $\pi^+$) with energy $T^*$, $F_{i,j}(h,T,T^*,\theta,\varphi)$ is the fluence of secondary particles of type $j$, produced by a primary CR particle of type $i$ (proton or $\alpha-$particle) with a given primary energy $T$ arriving at the top of the atmosphere from zenith angle $\theta$ and azimuth angle $\varphi$.

In the model, the conversion coefficients $C_j(T^*)$ are considered according to [66, 67]. We emphasize that employment of different conversion coefficients $C_j(T^*)$ would lead to an increase of the assessed exposure of about 20 %, which is considerably below the other model uncertainties [68, 69]. The model is in very good agreement with measurements, including stratospheric balloon-borne, reference data, as well as widely used models [65, 70–72].

An illustration of the application of the model within the full-chain analysis of NM data, namely deriving the SEP spectra-assessment of space weather effect, that is exposure at flight altitude during GLE is given in Fig.6a. Here, using the derived spectra during the peak intensity of SEPs of GLE #71, we computed the effective dose rate at L035, that is 35 kft. We would like to emphasize that the exposure during GLEs can reach peak values for a relatively short period, mostly corresponding to the peak SEP flux.

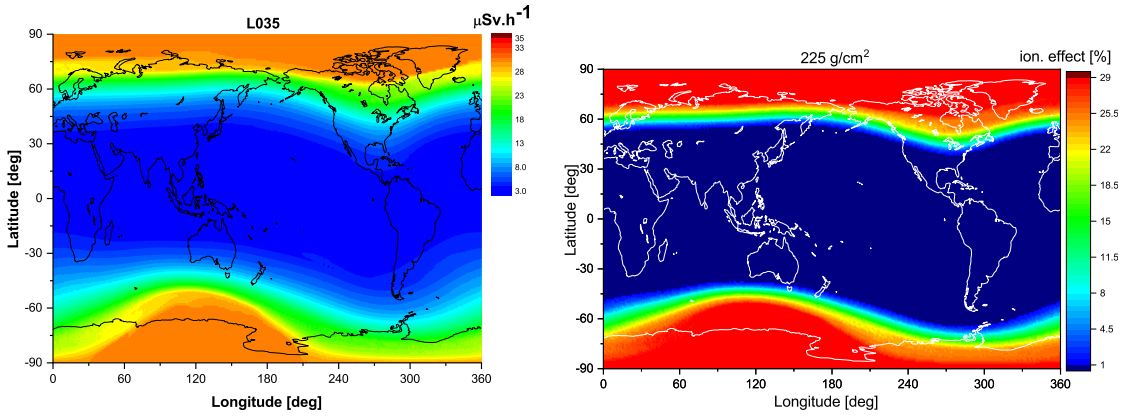


**(a)** The effective dose rate at L035 during the peak intensity of GLE # 71

**(b)** Ionization effect during the peak phase of GLE # 73 in the region of Regener-Pfotzer maximum.

**Figure 6:** Illustration of space weather and terrestrial effects during GLEs.

Despite the derived anisotropy, we conservatively assumed an isotropic angular distribution of the GLE particles similarly to [73, 74], considering also the event integrated angular distribution

Fig.4. As expected, the exposure is maximal in the polar region and significantly diminished at greater rigidity cut-off regions.

Similarly, employing a Monte Carlo based atmospheric ionization model [75] and the derived spectra during the GLE # 73 [39], the ion production rate at the region of Regener-Pfotzer maximum [76] can be computed, the details are given in Fig. 6b. We would like to emphasize that the ionization effects due to various populations of precipitating particles varies considerably from event to event [77, 78] and depends also on accompanying Forbush decreases, the latter could compensate the excess of ions produced by SEPs [79, 80].

## 5. Conclusions

Methodological observations and study of relativistic SEPs by various ground-based and space-borne instruments gives an unique opportunity to reveal their mechanism for accelerations, specifically in the tail of the spectrum, that is the high-energy range. The long-lasting paradigm of SEP acceleration by flare/CME for impulsive, gradual events respectively, was recently expanded by including hybrid and prolonged reconnection as discussed in this paper. The future development of the knowledge in the field and the open questions to be answered are related to clarifying the role of the ambient turbulence/waves and self-generated ones in the trapping and escape of SEPs during acceleration and transport in the corona and near the Sun. A specific interest shall be paid on how the coronal and interplanetary magnetic field affect the energization and escape of SEPs from their acceleration regions, which can be the key factor to the observed large event-to-event variations. Non the least what is the exact mechanism for triggering the SEP acceleration as well as the relative contribution of the different mechanisms should be answered. The ongoing space missions such as Parker Solar Probe and Solar Orbiter as well as the planned ones and the sustainable operation of the global NM network can provide the necessary observational material.

Finally, the precise quantification of the relativistic SEPs induced terrestrial effects is specifically important in order to provide reliable space weather service(s) and study the impact of energetic precipitating particles on atmospheric chemistry and physics.

Here, we reported and discussed several recent achievements of the aforementioned topics, specifically the physics and the related effects of relativistic SEPs/GLEs as well as the author's personal opinion of the future development of the field.

## Acknowledgements

The author warmly acknowledge the organizers of the ECRS 2022 for the invitation and possibility to give this talk. This work was supported by the Academy of Finland (project 330064 QUASARE and 321882 ESPERA) and the University of Oulu grant SARPEDON.

## References

[1] M. Desai and J. Giacalone, *Large gradual solar energetic particle events*, *Living Reviews in Solar Physics* **13** (2016), no. 1 3.

[2] O. Malandraki and N. Crosby, *Solar Particle Radiation Storms Forecasting and Analysis, The HESPERIA HORIZON 2020 Project and Beyond*, *Springer Nature* ASSL volume **444** (2018).

[3] M. Aschwanden, *GeV particle acceleration in solar flares and ground level enhancement (GLE) events*, *Space Science Reviews* **171** (2012), no. 1-4 3–21.

[4] M. Shea and D. Smart, *Possible evidence for a rigidity-dependent release of relativistic protons from the solar corona*, *Space Science Reviews* **32** (1982), 251–271.

[5] S. Poluianov, I. Usoskin, A. Mishev, A. Shea, and D. Smart, *GLE and sub-GLE redefinition in the light of high-altitude polar neutron monitors*, *Solar Physics* **292** (2017), no. 11 176.

[6] R. Vainio, L. Desorgher, D. Heynderickx, M. Storini, E. Flückiger, R. Horne, G. Kovaltsov, K. Kudela, M. Laurenza, S. McKenna-Lawlor, H. Rothkaehl and I. Usoskin, *Dynamics of the Earth's particle radiation environment*, *Space Science Reviews* **147** (2009), no. 3-4 187–231.

[7] L.I. Miroshnichenko, *Retrospective analysis of GLEs and estimates of radiation risks*, *Journal of Space Weather and Space Climate* **8** (2018), A52.

[8] A. Mishev, and P. Jiggens, *Preface to measurement, specification and forecasting of the Solar Energetic Particle (SEP) environment and Ground Level Enhancements (GLEs)*, *Journal of Space Weather and Space Climate* **9** (2019), E1.

[9] D. Reames, *Particle acceleration at the sun and in the heliosphere*, *Space Science Reviews* **90** (1999), 413–491.

[10] A. Anastasiadis et al., *Solar energetic particles in the inner heliosphere: Status and open questions*, *Philosophical Transactions of the Royal Society A: Mathematical, Physical and Engineering Sciences* **377** (2019), no. 2148 20180100.

[11] E. Vashenyuk, Y. Balabin, J. Perez-Peraza, A. Gallegos-Cruz and L. Miroshnichenko, *Some features of the sources of relativistic particles at the sun in the solar cycles 21-23*, *Advances Space Research* **38** (2006), no. 3 411–417.

[12] L. Kocharov, S. Pohjolainen, A. Mishev, M. Reiner, J. Lee, T. Laitinen, L. Didkovsky, V. Pizzo, R. Kim, A. Klassen, M. Karlicky, K.-S. Cho, D. Gary, I. Usoskin, E. Valtonen and R. Vainio, *Investigating the origins of two extreme solar particle events: Proton source profile and associated electromagnetic emissions*, *Astrophysical Journal* **839** (2017), no. 2 79.

[13] K-L. Klein, S. Musset, N. Vilmer, C. Briand, S. Krucker, A. Battaglia, N. Dresing, C. Palmroos, and D. Gary, *The relativistic solar particle event on 28 October 2021: Evidence of particle acceleration within and escape from the solar corona*, *Astronomy and Astrophysics* **663** (2022), A173.

[14] N. Mandzhavidze and R. Ramaty, *Gamma rays from pion decay - Evidence for long-term trapping of particles in solar flares*, *Astrophysical Journal Letters* **296** (1992), L111-L114.

[15] L. Kocharov, S. Pohjolainen, M.J. Reiner, A. Mishev, H. Wang, I. Usoskin and R. Vainio, *Spatial Organization of Seven Extreme Solar Energetic Particle Events*, *Astrophysical Journal Letters* **862** (2018), no. 2 L20.

[16] L. Kocharov, M. Pesce-Rollins, T. Latinen, A. Mishev et al., *Interplanetary Protons versus Interacting Protons in the 2017 September 10 Solar Eruptive Event* , *The Astrophysical Journal* **890** (2020), 13.

[17] A. Hutchinson, S. Dalla, T. Laitinen, G. de Nolfo, A. Bruno, J. Ryan, and C. Waterfall, *Energetic proton back-precipitation onto the solar atmosphere in relation to long-duration gamma-ray flares*, *Astronomy and Astrophysics* **658** (2022), A23.

[18] A. Mishev and S. Poluianov, *About the Altitude Profile of the Atmospheric Cut-Off of Cosmic Rays: New Revised Assessment*, *Solar Physics* **296** (2021), no. 8 129.

[19] J. Simpson. *The Cosmic Ray Nucleonic Component: The Invention and Scientific Uses of the Neutron Monitor*, *Space Science Reviews* **93** (2000), 11–32.

[20] A. Mishev and I. Usoskin, *Current status and possible extension of the global neutron monitor network*, *J. Space Weather Space Clim.* **10** (2020), 17.

[21] J. Bieber and P. Evenson, *Spaceship earth - an optimized network of neutron monitors*, in *Proc. of 24th ICRC Rome, Italy, 28 August - 8 September 1995*, vol. 4, pp. 1316–1319, 1995.

[22] H. Moraal and K. McCracken, *The time structure of ground level enhancements in solar cycle 23*, *Space Science Reviews* **171** (2012), no. 1-4 85–95.

[23] J. Cramp, M. Duldig, E. Flückiger, J. Humble, M. Shea and D. Smart, *The October 22, 1989,solar cosmic enhancement: ray an analysis the anisotropy spectral characteristics*, *Journal of Geophysical Research* **102** (1997), no. A11 24 237–24 248.

[24] D. Bombardieri, M. Duldig, K. Michael, and J. Humble, *Relativistic proton production during the 2000 July 14 solar event: The case for multiple source mechanisms* , *The Astrophysical Journal* **644** (2006), 565–574.

[25] A. Mishev, L. Kocharov and I. Usoskin, *Analysis of the ground level enhancement on 17 May 2012 using data from the global neutron monitor network*, *Journal of Geophysical Research* **119** (2014) 670–679.

[26] S.A. Koldobskiy, , V. Bindi, C. Corti, G. A. Kovaltsov, and I. G. Usoskin. *Validation of the Neutron Monitor Yield Function Using Data from AMS-02 Experiment 2011 – 2017*. *J. Geophys. Res. (Space Phys.)*, **124**, (2019) 2367–2379

[27] A.L. Mishev, S.A. Koldobskiy, G.A. Kovaltsov, A. Gil, and I.G. Usoskin. *Updated Neutron-Monitor Yield Function: Bridging Between In Situ and Ground-Based Cosmic Ray Measurements*. *J. Geophys. Res. (Space Phys.)*, **125** (2020), e2019JA027,433.

[28] A. Tikhonov, A. Goncharsky, V. Stepanov and A. Yagola, *Numerical Methods for Solving ill-Posed Problems*. Kluwer Academic Publishers, Dordrecht, 1995.

[29] S. Mavrodiev, A. Mishev and J. Stamenov, *A method for energy estimation and mass composition determination of primary cosmic rays at the Chacaltaya observation level based on the atmospheric Cherenkov light technique*, *Nucl. Instr. and Methods in Phys. Res. A* **530** (2004), no. 3 359–366.

[30] A. Mishev , S. Mavrodiev, and J. Stamenov, *Gamma rays studies based on atmospheric Cherenkov technique at high mountain altitude*, *International Journal of Modern Physics A* **20** (2005), no. 29 7016–7019.

[31] K. Levenberg, *A method for the solution of certain non-linear problems in least squares*, *Quarterly of Applied Mathematics* **2** (1944) 164–168.

[32] D. Marquardt, *An algorithm for least-squares estimation of nonlinear parameters*, *SIAM Journal on Applied Mathematics* **11** (1963), no. 2 431–441.

[33] A. Gil, I. Usoskin, G. Kovaltsov, A. Mishev, C. Corti and V. Bindi, *Can we properly model the neutron monitor count rate?*, *J. Geophys. Res.* **120** (2015) 7172–7178.

[34] P.-S. Mangeard, D. Ruffolo, A. Sáiz, W. Nuntiyakul, J. Bieber, J. Clem, P. Evenson, R. Pyle, M. Duldig and J. Humble, *Dependence of the neutron monitor count rate and time delay distribution on the rigidity spectrum of primary cosmic rays*, *Journal of Geophysical Research: Space Physics* **121** (2016), no. 12 11,620–11,636.

[35] W. Nuntiyakul, A. Sáiz, D. Ruffolo, P.-S. Mangeard, P. Evenson, J. Bieber, J. Clem, R. Pyle, M. Duldig and J. Humble, *Bare neutron counter and neutron monitor response to cosmic rays during a 1995 latitude survey*, *Journal of Geophysical Research: Space Physics* **123** (2018), no. 9 7181–7195.

[36] A. Mishev, I. Usoskin, O. Raukunen, M. Paassilta, E. Valtonen, L. Kocharov and R. Vainio, *First analysis of GLE 72 event on 10 September 2017: Spectral and anisotropy characteristics*, *Solar Physics* **293** (2018) 136.

[37] A. Mishev, S. Koldobskiy, L. Kocharov and I. Usoskin, *GLE # 67 Event on 2 November 2003: An Analysis of the Spectral and Anisotropy Characteristics Using Verified Yield Function and Detrended Neutron Monitor Data*, *Solar Physics* **296** no. 5 (2021) 79.

[38] A. Mishev, S. Koldobskiy, I. Usoskin, L. Kocharov and G. Kovaltsov, *Application of the verified neutron monitor yield function for an extended analysis of the GLE # 71 on 17 May 2012*, *Space Weather* **19** no. 2 (2021) e2020SW002626.

[39] A. Mishev, L. Kocharov, S. Koldobskiy, N. Larsen, E. Riihonen, R. Vainio and I. Usoskin, *High-Resolution Spectral and Anisotropy Characteristics of Solar Protons During the GLE N 73 on 28 October 2021 Derived with Neutron-Monitor Data Analysis*, *Solar Physics* **297** no. 5 (2022) 88.

[40] A. Papaioannou, A. Kouloumvakos, A. Mishev, R. Vainio, I. Usoskin, et al., *The first ground level enhancement of solar cycle 25 on 28 October 2021*, *Astronomy and Astrophysics* **660** (2022), L5.

[41] J. Clem, *Contribution of Obliquely Incident particles to Neutron Monitor Counting Rate*, *Journal of Geophysical Research* **102** (1997), 919.

[42] A. Mishev and I. Usoskin, *Analysis of the ground level enhancements on 14 July 2000 and on 13 December 2006 using neutron monitor data*, *Solar Physics* **291** (2016), no. 4 1225–1239.

[43] R. Caballero-Lopez and H. Moraal, *Limitations of the force field equation to describe cosmic ray modulation*, *Journal of Geophysical Research* **109** (2004) A01101.

[44] E. Vos and M. Potgieter, *New modeling of galactic proton modulation during the minimum of solar cycle 23/24*, *Astrophysical Journal* **815** (2015), 119.

[45] I. Usoskin, G. Bazilevskaya, and G. Kovaltsov, *Solar modulation parameter for cosmic rays since 1936 reconstructed from ground-based neutron monitors and ionization chambers*, *Journal of Geophysical Research* **116** (2011) A02104.

[46] J. Cramp, J. Humble, and M. Duldig, *The cosmic ray ground-level enhancement of 24 October 1989*, *Proc. Astronom. Soc. Australia* **11** (1995) 28.

[47] N. Larsen, A. Mishev and I. Usoskin *Development of a Modern Open Source Magnetospheric Computation Tool* , *Proceeding of Science* **This proceedings** (2022).

[48] P. Alken, E. Thebault, C. Beggan, H. Amit, J. Aubert et al., *International Geomagnetic Reference Field: the thirteenth generation*, *Earth, Planets and Space* **73** (2021), no. 1 49.

[49] N. Tsyganenko, *A magnetospheric magnetic field model with a warped tail current sheet*, *Planetary and Space Science* **37** (1989), no. 1 5–20.

[50] K. Kudela and I. Usoskin, *On magnetospheric transmissivity of cosmic rays*, *Czechoslovak Journal of Physics* **54** (2004), no. 2 239–254.

[51] J. Nevalainen, I. Usoskin, and A. Mishev, *Eccentric dipole approximation of the geomagnetic field: Application to cosmic ray computations*, *Advances in Space Research* **52** (2013), no. 1 22–29.

[52] D. Himmelblau, *Applied Nonlinear Programming*. Mcgraw-Hill(Tx), 1972.

[53] R. Bütikofer and E. Flückiger, *Differences in published characteristics of GLE 60 and their consequences on computed radiation dose rates along selected flight paths*, *Journal of Physics: Conference Series* **409** (2013), no. 1 012166.

[54] A. Mishev, L. Kocharov, S. Koldobskiy, N. Larsen, E. Riihonen, et al., *The first GLE (# 73 – 28-Oct-2021) of solar cycle 25: study using space-borne and NM data*, *Proceeding of Science* **This proceedings** (2022).

[55] A. Bruno, G. Bazilevskaya, M. Boezio, E. Christian, G. Nolfo, et al., *Solar energetic particle events observed by the PAMELA mission*, *Astrophysical Journal* **862** (2018), no. 2 97.

[56] O. Adriani, G. Barbarino, G. Bazilevskaya, R. Bellotti, M. Boezio, et al., *PAMELA's measurements of magnetospheric effects on high-energy solar particles*, *Astrophysical Journal Letters* **801** (2015), no. 1 L3.

[57] P. Kühl, S. Banjac, N. Dresing, R. Goméz-Herrero, B. Heber, A. Klassen, and C. Terasa, *Proton intensity spectra during the solar energetic particle events of May 17, 2012 and January 6, 2014*, *Astronomy and Astrophysics* **576** (2015), A120.

[58] M. Shea and D. Smart, *Cosmic ray implications for human health*, *Space Science Reviews* **93** (2000), no. 1-2 187–205.

[59] A. Ferrari, M. Pelliccioni, and T. Rancati, *Calculation of the radiation environment caused by galactic cosmic rays for determining air crew exposure*, *Radiation Protection Dosimetry* **93** (2001), no. 2 101–114.

[60] S. Roesler, W. Heinrich, and H. Schraube, *Monte Carlo calculation of the radiation field at aircraft altitudes*, *Radiation Protection Dosimetry* **98** (2002), no. 4 367–388.

[61] T. Sato, H. Yasuda, K. Niita, A. Endo, and L. Sihver, *Development of parma: Phits-based analytical radiation model in the atmosphere*, *Radiation Protection Dosimetry* **170** (2008) 244–259.

[62] J. Bottollier-Depois, P. Beck, B. Bennett, L. Bennett, R. Bütikofer, et al., *Comparison of codes assessing galactic cosmic radiation exposure of aircraft crew,* , *Radiation Research* **136** (2009) 317–323.

[63] S. Tuohino, A. Ibragimov, I. Usoskin and A. Mishev, *Upgrade of GLE database: Assessment of effective dose rate at flight altitude*, *Advances in Space Research* **62** (2018), no. 2 398–407.

[64] A. Mishev and I. Usoskin, *Numerical model for computation of effective and ambient dose equivalent at flight altitudes. application for dose assessment during gles*, *Journal of Space Weather and Space Climate* **5** (2015) A10.

[65] A. Mishev, S. Tuohino and I. Usoskin, *Neutron monitor count rate increase as a proxy for dose rate assessment at aviation altitudes during GLEs*, *J. Space Weather Space Clim.* **8** (2018) A46.

[66] N. Petoussi-Henss, W. Bolch, K. Eckerman, A. Endo, N. Hertel, J. Hunt, M. Pelliccioni, H. Schlattl, and M. Zankl, *Conversion coefficients for radiological protection quantities for external radiation exposures*, *Annals of the ICRP* **40** (2010), no. 2-5 1–257.

[67] M. Pelliccioni, *Overview of fluence-to-effective dose and fluence-to-ambient dose equivalent conversion coefficients for high energy radiation calculated using the Fluka code*, *Radiation Protection Dosimetry* **88** (2000), no. 4 279–297.

[68] K. Copeland, and W. Atwell *Flight safety implications of the extreme solar proton event of 23 February 1956*, *Advances in Space Research* **63** (2019), no. 1 665–671.

[69] Z. Yang, and R. Sheu *An in-depth analysis of aviation route doses for the longest distance flight from Taiwan*, *Radiation Physics and Chemistry* **168** (2020), 108,548.

[70] H. Menzel, *The international commission on radiation units and measurements*, *Journal of the ICRU* **10** (2010), no. 2 1–35.

[71] M. Meier, M. Hubiak, D. Matthiä, M. Wirtz, and G. Reitz, *Dosimetry at aviation altitudes (2006-2008)*, *Radiation Protection Dosimetry* **136** (2009), no. 4 1–35.

[72] A. Mishev, A. Binios, E. Turunen et al., *Measurements of natural radiation with an MDU Liulin type device at ground and in the atmosphere at various conditions in the Arctic region*, *Radiation Measurements* **154** (2022) 106757.

[73] K. Copeland, H. Sauer, F. Duke, and W. Friedberg, *Cosmic radiation exposure of aircraft occupants on simulated high-latitude flights during solar proton events from 1 January 1986 through 1 January 2008*, *Advances in Space Research* **42** (2008), no. 6 1008–1029.

[74] A. Mishev, and I. Usoskin, *Assessment of the radiation environment at commercial jet-flight altitudes during GLE 72 on 10 September 2017 using neutron monitor data*, *Space Weather* **16** (2018), no. 12 1921–1929.

[75] P. Velinov, S. Asenovski, K. Kudela, J. Lastovička, L. Mateev, A. Mishev and P. Tonev, *Impact of cosmic rays and solar energetic particles on the Earth's ionosphere and atmosphere*, *Journal of Space Weather and Space Climate* **3** (2013) A14.

[76] E. Regener and G. Pfotzer, *Vertical intensity of cosmic rays by threefold coincidences in the stratosphere*, *Nature* **136** (1935) 718–719.

[77] A. Mishev and P. Velinov, *Time evolution of ionization effect due to cosmic rays in terrestrial atmosphere during GLE 70*, *Journal of Atmospheric and Solar-Terrestrial Physics* **129** (2015) 78–86.

[78] A. Mishev and P. Velinov, *Ion production and ionization effect in the atmosphere during the Bastille day GLE 59 due to high energy SEPs*, *Advances in Space Research* **61** (2018), no. 1 316–325.

[79] A. Mishev and P. Velinov, *Ionization effect in the Earth's atmosphere during the sequence of October–November 2003 Halloween GLE events*, *Journal of Atmospheric and Solar-Terrestrial Physics* **211** (2020), 105484.

[80] L. Dorman, A. Mishev and P. Velinov, *Global planetary ionization maps in Regener-Pfotzer cosmic ray maximum for GLE 66 during magnetic superstorm of 29–31 October 2003*, *Advances in Space Research* **70** (2022), no. 9 253-260.